

Tied Block Convolution: Leaner and Better CNNs with Shared Thinner Filters

Xudong Wang^{1,2} and Stella X. Yu^{1,2}

¹ University of California, Berkeley

² International Computer Science Institute

xdwang@eecs.berkeley.edu, stellayu@berkeley.edu

Abstract

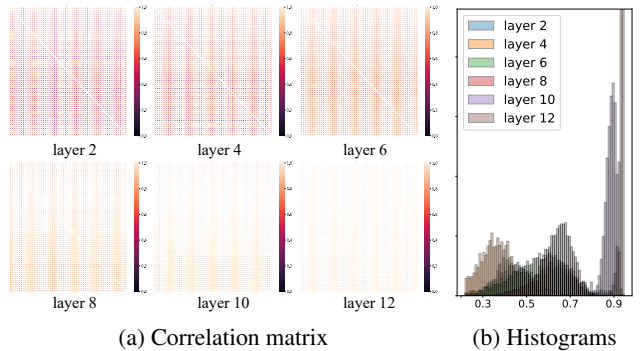
Convolution is the main building block of convolutional neural networks (CNN). We observe that an optimized CNN often has highly correlated filters as the number of channels increases with depth, reducing the expressive power of feature representations. We propose *Tied Block Convolution* (TBC) that shares the same thinner filters over equal blocks of channels and produces multiple responses with a single filter. The concept of TBC can also be extended to group convolution and fully connected layers, and can be applied to various backbone networks and attention modules.

Our extensive experimentation on classification, detection, instance segmentation, and attention demonstrates TBC’s significant across-the-board gain over standard convolution and group convolution. The proposed TiedSE attention module can even use $64\times$ fewer parameters than the SE module to achieve comparable performance. In particular, standard CNNs often fail to accurately aggregate information in the presence of occlusion and result in multiple redundant partial object proposals. By sharing filters across channels, TBC reduces correlation and can effectively handle highly overlapping instances. TBC increases the average precision for object detection on MS-COCO by 6% when the occlusion ratio is 80%. Our code will be released.

Introduction

Convolution is the main building block of convolutional neural networks (CNN), which are widely successful on image classification (Krizhevsky, Sutskever, and Hinton 2012; He et al. 2016; Xie et al. 2017; Simonyan and Zisserman 2014), object detection (Girshick 2015; Ren et al. 2015; He et al. 2017), image segmentation (Kirillov et al. 2019; Long, Shelhamer, and Darrell 2015; Chen et al. 2017, 2018) and action recognition (Ji et al. 2012; Wang et al. 2016; Carreira and Zisserman 2017; Wang et al. 2018). However, standard convolution is still costly in terms of computation, storage, and memory access. More importantly, an optimized CNN often develops highly correlated filters.

We can evaluate pairwise filter similarity in standard convolution (SC), using the cosine similarity of guided backpropagation patterns (Springenberg et al. 2014) averaged over a set of ImageNet images. Fig. 1 shows that, as the depth of layer increases, the filter correlation also increases. That is, filters become more similar from early to late layers, reducing the expressive power of feature representations.



(a) Correlation matrix

(b) Histograms

Figure 1: (a) **Correlation matrix of 64 randomly selected filters** from layer 2 to layer 12 of VGG16. At depth layer d of VGG16 for ImageNet classification, we compute the similarity between two filters based on their guided backpropagation patterns (Springenberg et al. 2014) averaged on a set of images. As the layers get deeper, it becomes easier to find a set of filters that have a high similarity score to each other. (b) **Normalized histograms of pairwise filter similarities** of various VGG16 layers. As the number of channels increases with depth from 64 to 128 to 256, the curve shifts right and becomes far narrower, i.e., more filters become similar. Motivated by this, *can we eliminate redundancy in the convolution layer by reusing similar filters?*

How to optimize a CNN with less redundancy has been studied (Howard et al. 2017; Zhang et al. 2018; Ma et al. 2018; Xie et al. 2017), often by exploring dependencies across space and channel dimensions. In SC, while each filter has a limited size spatially, it extends to the full set of input features, whereas in group convolution (GC) (Krizhevsky, Sutskever, and Hinton 2012), a filter only convolves with a subset of input features. Therefore, if there are B groups of input features, each GC layer reduces the number of parameters B times by reducing the size of each filter by B times. Depth-wise convolution (DW) is an extreme case of GC, where each group only contains one channel, maximally reducing the parameter count.

While GC and DW are effective at reducing the model size, they do not look into the correlation between filters and their isolated representations cannot capture cross-channel relationships. Instead of removing redundancy by reducing the size of each filter as in GC and DW, we explore an-

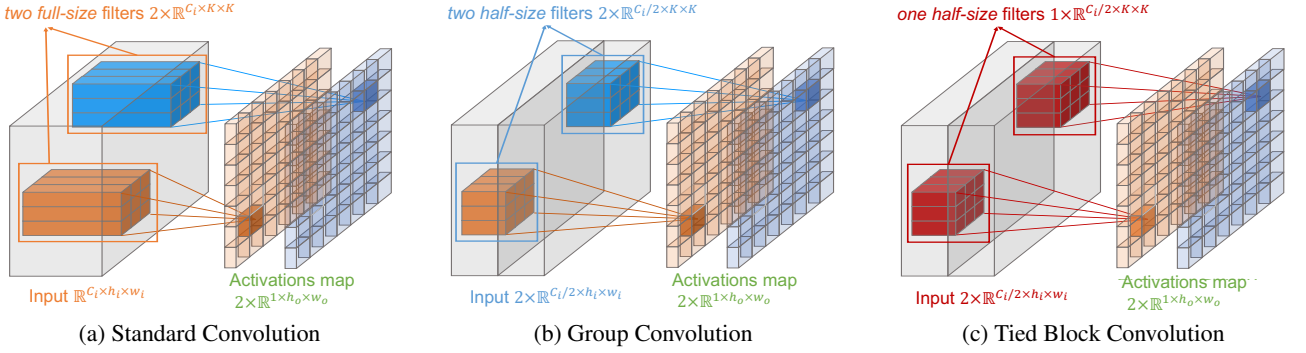


Figure 2: **Convolution operators.** To generate two activation maps, standard convolution requires *two full-size filters* and group convolution requires *two half-size filters*, however, our tied block convolution only requires *one half-size filter*, that is, the parameters are reduced by $4\times$. The idea of TBC can also be applied to fully connected and group convolutional layers.

other way of eliminating redundancy by exploring the potential of each filter. Directly reducing the number of filters is known to reduce the model capacity (He et al. 2016). However, since SC filters become similar (Fig. 1), we can reduce the *effective number* of filters by reusing them across different feature groups. We propose such a simple alternative called *tied block convolution* (TBC): We split C input feature channels into B equal blocks, and use a single block filter defined only on $\frac{C}{B}$ channels to produce B responses. Fig. 2 shows that an SC filter spans the entire C channels, whereas at $B = 2$, our TBC spans only $\frac{C}{2}$ channels and yet it also produces 2 filter responses. TBC is simply GC shared across groups, and TBC is reduced to SC when $B=1$. The tied block group convolution (TGC) and tied block fully connected layer (TFC) can be straightforwardly obtained by extending this concept to fully connected layer and group convolution layer.

Our TBC utilizes each filter, memory access, and samples more effectively. **1)** At $B = 2$, TBC obtains the same number of responses with one half-sized thin filter, approaching the same SC-size output with 4 times of model reduction. **2)** As the same thin filter is applied to each of the B blocks, TBC has more efficient memory access by utilizing GPU parallel processing. **3)** Since each thin filter is trained on B times more samples, learning also becomes more effective. **4)** Since each set of TBC filters are applied to all input channels, TBC could aggregate global information across channels and better model cross-channel dependencies.

While TBC seems to be an appealing concept in theory, whether we can demonstrate its advantage in practice over SC or GC would be critically dependent upon neural network architectures. We apply TBC/TGC/TFC to various backbone networks, including ResNet (He et al. 2016), ResNeXt (Xie et al. 2017), SENet (Hu, Shen, and Sun 2018) and ResNeSt (Zhang et al. 2020), and propose their tied version: *TiedResNet*, *TiedResNeXt*, *TiedSENet* and *TiedResNeSt*. Extensive experimentation on classification, detection, segmentation, and attention are conducted, which demonstrate TBC/TGC/TFC’s significant across-the-board performance improvement over *standard convolution*, *group convolution* and fully connected layer. For example, Fig. 6 shows TiedResNet consistently outperforms ResNet, ResNeXt and HRNetV2 (Wang et al. 2019) by a larger mar-

gin with a much leaner model. Similar performance boost and model reduction are also obtained in various frameworks, tasks and datasets.

Lastly, learned filter redundancy not only reduces the model capacity at a bloated size, but also renders the CNN unable to capture diversity, resulting in inferior performance. For object detection on MS-COCO, standard CNNs often fail to accurately locate the target object regions and aggregate useful information from the foreground. Consequently, there are multiple overlapping partial object proposals, preventing a single full object proposal to emerge from the proposal pool. TiedResNet can handle high overlapping instances much better and increase the average precision (AP) by 6% and AP at IoU = 0.75 by 8.3%, when the occlusion ratio is 0.8.

Related works

Backbone Networks. AlexNet (Krizhevsky, Sutskever, and Hinton 2012) is the first CNN success with significant accuracy gain on the ILSVRC competition. However, large kernels and fully connected layers greatly increase the model size. With smaller kernels, GoogleNet (Szegedy et al. 2015) and VGGNet (Simonyan and Zisserman 2014) only need 12 times fewer parameters to outperform (Krizhevsky, Sutskever, and Hinton 2012; Zeiler and Fergus 2014). However, the large network depth causes vanishing gradient problems, which is later solved by the residual connection design in ResNet (He et al. 2016). Since the depth of model is no longer an issue, researchers have begun to explore how to use parameters more efficiently. With comparable model complexity, ResNeXt (Xie et al. 2017) outperforms ResNet in many major tasks, mainly due to the use of efficient group convolution. Through careful design of the architecture, HRNetV2 (Wang et al. 2019) achieves the state-of-the-art performance on multiple major tasks. Compared with these works using either GC or SC, Our TBC further utilizes the full potential of each thinner filter. We provide comparisons with these networks in remaining sections.

Group-wise Convolution. Group convolution (GC) (Krizhevsky, Sutskever, and Hinton 2012) is proposed to remove filter redundancy. Since each GC filter only convolves with features in its group, with the same number of channels, this mechanism can reduce the number of

parameters in each layer by a factor of B , where B is the number of groups. When the number of groups is the same as the number of input features, GC becomes identical to depth-wise convolution (DW) (Howard et al. 2017). Both GC and DW greatly reduce the model redundancy by reducing the size of each filter. *However, they never look into the correlation between (learned) filters.*

As each filter in GC and DW only responds to partial input feature map, the ability to incorporate global information across channel dimensions is damaged in the GC and completely lost in the DW. In contrast, our TBC filter is shared across all input channels, and the long-range dependencies can be aggregated. This mechanism also introduces another benefit, our TBC only has one fragmentation. Therefore, TBC can take full advantage of the powerful parallel computing capabilities of the GPU.

Attention Modules. (Hu, Shen, and Sun 2018) introduces the squeeze-and-excitation (SE) module to adaptatively recalibrate channel-wise feature responses. (Cao et al. 2019) unifies SE and a non-local (Wang et al. 2018) module into a global context block (GCB). While SE and GCB are relatively light, SE (GCB) still counts for 10% (25%) of the model size. Our tied block convolution and tied fully connected layers can be integrated into various attention modules and significantly reduce the number of parameters: 2.53M vs 0.04M for SE and 10M vs 2.5M for GCB.

Tied Block Convolution Network Design

We first analyze TBC and TGC to guide us in network design. We also develop TFC and apply to attention modules.

TBC Formulation

Let the input feature be denoted by $X \in \mathbb{R}^{c_i \times h_i \times w_i}$ and the output feature $\tilde{X} \in \mathbb{R}^{c_o \times h_o \times w_o}$, where c, h, w are the number of channels, the height and width of feature maps respectively. The kernel size is $k \times k$ and the bias term is ignored for clarity.

Standard Convolution, denoted by $*$, can be formulated as:

$$\tilde{X} = X * W \quad (1)$$

where $W \in \mathbb{R}^{c_o \times c_i \times k \times k}$ is the SC kernel. The parameters for SC is thus: $c_o \times c_i \times k \times k$.

Group Convolution first divides input feature X into G equal-sized groups X_1, \dots, X_G with size $c_i/G \times h_i \times w_i$ per group. Each group shares the same convolutional filters W_g . The output of GC is computed as:

$$\tilde{X} = X_1 * W_1 \oplus X_2 * W_2 \oplus \dots \oplus X_G * W_G \quad (2)$$

where \oplus is the concatenation operation along the channel dimension, W_g is the convolution filters for group g , where $g \in \{1, \dots, G\}$, $W_g \in \mathbb{R}^{\frac{c_o}{G} \times \frac{c_i}{G} \times k \times k}$. The number of parameters for GC is: $G \times \frac{c_o}{G} \times \frac{c_i}{G} \times k \times k$.

Tied Block Convolution reduces the *effective number* of filters by reusing filters across different feature groups with the following formula:

$$\tilde{X} = X_1 * W' \oplus X_2 * W' \oplus \dots \oplus X_B * W' \quad (3)$$

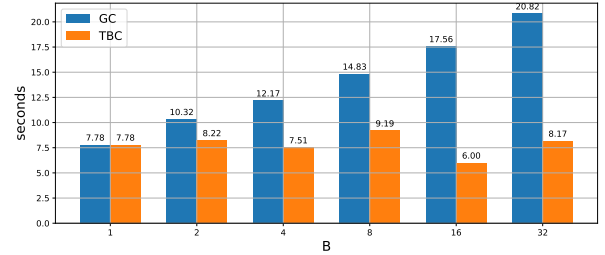


Figure 3: **The time cost of processing 1k iterations** of each feature map using the RTX 2080Ti GPU. When group number increases, GC increases the time cost almost linearly. In contrast, when using a larger B , TBC keeps a similar time cost. Different block numbers B were tested for GC and TBC, the total FLOPs at these values were fixed by changing the total filter number. When $B = 1$, GC and TBC are equal to SC. Input feature map size is $56 \times 56 \times 2048$.

where $W' \in \mathbb{R}^{\frac{c_o}{B} \times \frac{c_i}{B} \times k \times k}$ is the TBC filters shared among all the groups. The parameter number is: $\frac{c_o}{B} \times \frac{c_i}{B} \times k \times k$.

TBC vs. GC. While TBC is GC with filters shared across groups, it has several major distinctions from GC in practical consequences (assume $B = G$).

1. TBC has $B \times$ fewer parameters than GC.
2. TBC only has one fragmentation on GPU utilization, whereas GC has G fragmentations, greatly reducing the degree of parallelism. Fig.3 shows that the processing time increases linearly with the number of groups in GC, whereas our TBC keeps almost the same processing time.
3. TBC can better model cross-channel dependencies. Since each set of GC filters are only convolved on subsets of channels, GC has trouble aggregating global information across channels. However, each set of TBC filters are applied to all input channels and can better model cross-channel dependencies.
4. TBC-based TiedResNet greatly surpasses GC-integrated ResNeXt in object detection and instance segmentation tasks. TiedResNet-S can even outperform ResNeXt with $2 \times$ model size reduction, demonstrating that TiedResNet make more effective use of model parameters.

Tied Block Group Convolution (TGC) The idea of tied block filtering can also be directly applied to group convolution, formulated as:

$$\tilde{X} = (X_{11} * W'_1 \oplus \dots \oplus X_{1B} * W'_1) \oplus \dots \oplus (X_{G1} * W'_G \oplus \dots \oplus X_{GB} * W'_G) \quad (4)$$

where $W'_g \in \mathbb{R}^{\frac{c_o}{BG} \times \frac{c_i}{BG} \times k \times k}$, $X_{gb} \in \mathbb{R}^{\frac{c_i}{BG} \times h_i \times w_i}$ is the divided feature map, $g \in [1, G]$ and $b \in [1, B]$.

Tied Block Fully Connected Layer (TFC) Convolution is a special case of fully connected (FC) layer, just as FC is a special case of convolution. We apply the same tied block filtering idea to FC. Tied block fully connected layer (TFC) shares the FC connections between equal blocks of input channels. Like TBC, TFC could reduce B^2 times parameters and B times computational cost.

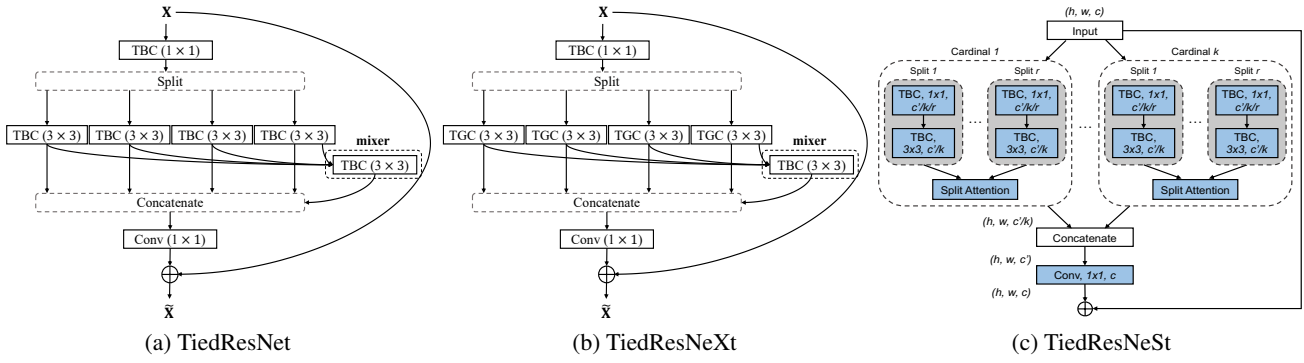


Figure 4: **Diagram of bottleneck modules** for (a) TiedResNet with 4 splits (b) TiedResNeXt with 4 splits and (c) TiedResNeSt. Each tied block convolution (TBC) and tied block group convolution (TGC) has a specific block number.

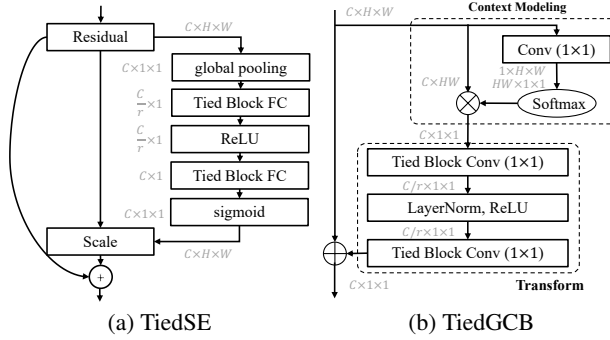


Figure 5: **Diagram of Tied attention modules.** (a) TiedSE module replaces FC in the original squeeze-and-excitation (SE) module (Hu, Shen, and Sun 2018) to be TFC. (b) TiedGCB module replaces standard convolution in global context block (GCB) (Cao et al. 2019) with TBC.

TBC/TGC in Bottleneck Modules

The ResNet/ResNeXt/ResNeSt bottleneck modules have 1×1 and 3×3 convolutional filters. We apply TBC/TGC differently as in Fig.4. For 3×3 in ResNet and ResNeXt, we split all the filters into groups; each group has its own TBC/TGC setting. This choice allows different levels of sharing and is motivated by network visualization works (Zeiler and Fergus 2014; Bau et al. 2017): Filters assume different roles at different layers and some are unique concept detectors (Agrawal, Carreira, and Malik 2015; Bau et al. 2017). For the 1×1 convolutions at the entry and the exit of bottlenecks, we replace the entry one by TBC with $B = 2$ to allow filter sharing, while maintaining the exit convolution to aggregate information across channels. Since ResNeSt replaces 3×3 convolutions to be multi-path and split attention modules with k cardinals, 3×3 convolutions occupy less proportion of the overall model complexity. Therefore, we only replace all 3×3 convolution to be TBC with $B = 2$ as in 1×1 convolution. Further increase of B will only marginally reduce the model parameters, but will greatly reduce performance.

The default setting for TiedResNet-50 (TiedResNeXt-50) is 4 splits with base width of 32 (64), i.e. $4s \times 32w$ ($4s \times 64w$), and the default setting for TiedResNet-S (TiedResNeXt-50-S) is $4s \times 18w$ ($4s \times 36w$). Our TiedBottleNeck reaches more than 1% performance improvement in term of top-1 accuracy

on ImageNet-1K. However, losing cross-channel integration could weaken the model. To add it back, we introduce a mixer that fuses outputs of multiple splits. Introducing the mixer increases performance by another 0.5%. The input to the mixer can be either concatenation or element-wise sum of split outputs. Table 6 shows that element-wise sum has a better trade-off.

TBC and TFC in Attention Modules

We apply TBC and TFC to attention modules such as SE (Hu, Shen, and Sun 2018) and GCB (Cao et al. 2019), by simply replacing SC and FC with their tied block counterparts (Fig. 5). Both designs significantly reduce the number of parameters without dropping performance.

Experimental Results

We conduct extensive tests of TBC, TGC and TFC on major benchmarks for object recognition, object detection, instance segmentation and attention.

ImageNet Classification

Implementation. We follow standard practices and perform data augmentation with random cropping to size 224×224 pixels (He et al. 2016). We train the network using SGD with a momentum of 0.9 and a mini-batch of 256 on 8 GPUs. The learning rate is initially set to 0.1 and then decayed $10 \times$ every 30 epochs for a total of 100 epochs.

Performance gain. Table 1 compares the recognition accuracy of multiple models on ImageNet-1k (Deng et al. 2009) validation set. In Table 1, TiedResNet50-S beats ResNet50 in terms of top-1 accuracy with only 60% flops and 54% parameters, likewise for TiedResNet101-S. With similar model complexity, TiedResNet50 and TiedResNet101 can beat benchmarks by more than 1.5% and 1.4% separately with 10% parameter reduction. Similar tendency can be observed for TiedResNeXt and TiedSENet. To further prove the effectiveness of TBC, we integrate it with current SOTA model ResNeSt. With only 59% of parameters and 82% of computation cost, TiedResNeSt-50-S obtains better performance than ResNeSt-50-S on ImageNet-1k.

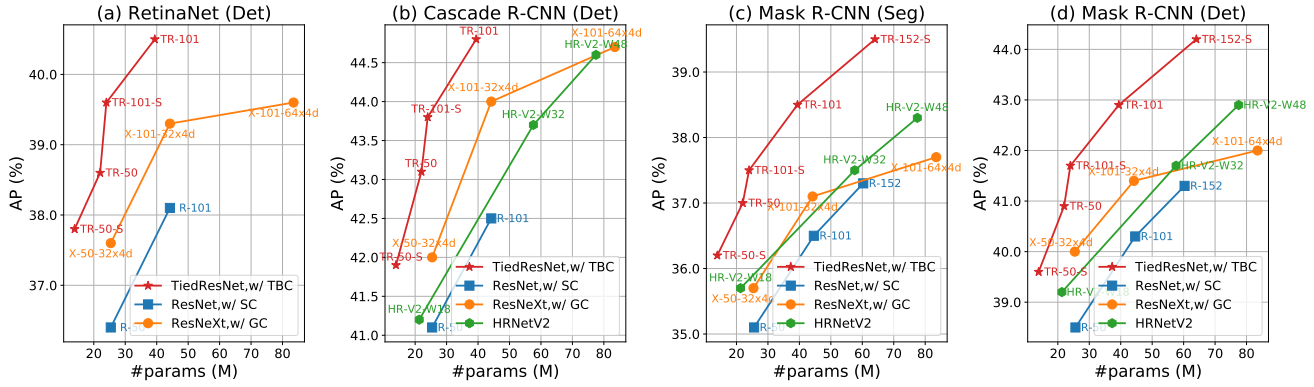


Figure 6: #params of backbones vs. their Average Precision on **object detection and instance segmentation tasks of MS-COCO val-2017**. For *single-stage* detector RetinaNet and *two-stage* detectors Cascade R-CNN and Mask R-CNN, TiedResNet consistently outperforms ResNet, ResNeXt and HRNetV2 with much fewer parameters. Detailed results are in appendix.

Object Detection and Instance Segmentation

MS-COCO (Lin et al. 2014) consists of 80 object categories with 118K/5K/208K images for training (*train-2017*), validation (*val-2017*) and testing (*test-2017*) respectively. Average Precision (AP) across IoU thresholds from 0.5 to 0.95 with an interval of 0.05 is evaluated. Detection performance at various qualities, AP_{50} and AP_{75} , and at different scales, AP_S , AP_M and AP_L , are reported. All models are trained on *train-2017* split and results reported on *val-2017*.

Implementation. We use baseline backbones and our TiedResNet model in PyTorch implemented (Chen et al. 2019) detectors. The long and short edges of images are resized to a maximum of 1333 and 800 respectively without changing the aspect ratio. Since 1× learning schedule (LS) is under-sutured, we only report results on 2× LS for both baselines and our models.

Results. We conduct thorough comparisons with ResNeXt and ResNet on multiple state-of-the-art frameworks including single-stage detector, RetinaNet (Lin et al. 2017), and two-stage detectors and Mask R-CNN (He et al. 2017) as in Fig.6. Since (Chen et al. 2019) re-implemented results are generally better than those in the original papers, we report re-implemented results for fair comparisons.

Object detection. As in Fig.6, using TiedResNet as backbone, single-stage detector RestinaNet and two-stage detector Cascade R-CNN and Mask R-CNN consistently outperform baselines by 2% to 2.5% in terms of box AP. TiedResNet101 on RetinaNet even greatly outperforms the much heavier-weight ResNeXt101-64×4d. Detailed comparison on various frameworks and Pascal VOC (Everingham et al. 2015) are in appendix materials.

Instance segmentation. With light-weight TiedResNet-S and comparable sized TiedResNet backbones, we observe an increase in AP^{mask} by 1.1% and 2.1% respectively. No matter how strong the baseline detector is, we always observe a boost in AP, corroborating the effectiveness of TBC.

Highly occluded Instances. Since occlusion requires the network to accurately detect the target area and distinguish different instances at the same time, the performance on images with large occlusion reveals the network’s localization

capabilities. The occlusion ratio (r) of each image is:

$$r = \frac{\text{total overlap area}}{\text{total instance area}} \quad (5)$$

The AP averaged over IoU 0.5 to 0.95, and at IoU=0.75, AP^{75} , are used as standard and restricted evaluation metrics respectively. Fig.7a and Fig.7b shows that ResNet is greatly affected by occlusion, AP^{75} drops by more than 6% at $r = 0.8$, whereas our TiedResNet only slightly decreases by 0.7%, exceeding the baseline of 8.3%. Similarly, as the occlusion rate becomes larger, the improvement on AP increases from 2.8% to 5.9%. These quantitative results in MS-COCO indicate TiedResNet’s strong capability of handling highly overlapping instances, especially on restricted evaluation metric. Fig.7c shows that TiedResNet has fewer false positive proposals and better segmentation quality.

Why larger gain on single-stage detector? Fig.A.1 shows that TiedResNet localizes the target area much better than ResNet/ResNeXt, which is especially beneficial for a single-stage detector that does not have a proposal regression layer.

Performance on Cityscapes. Since Cityscapes (Cordts et al. 2016) is a small dataset, thus deeper networks will generally overfit it. Therefore, we only deploy experiments with 50 layers backbone for Cityscapes datasets. Table 2 shows that TiedResNet50 can reach 2.1% gain for AP^{mask} .

Lightweight Attention

Fig. 5 shows our lightweight attention modules. The SE module can be seen as a special case of our TiedSE when $B=1$; likewise, GCB is TiedGCB at $B=1$.

Results of TiedSE. All experiments in Table 3 use reduction ratio of 16 for both baseline and our model. Several hyper-parameter settings of our TFC layer are investigated. Since our re-implemented baseline results are better than those in (Hu, Shen, and Sun 2018), we report our results for fair comparison. While SE is light weight, it still incurs 10% parameters of overall model. Table 3 shows that, at $B=8$, with 64× parameters reduction, TiedSE still obtains comparable performance. TiedSE significantly reduces parameters without sacrificing performance not only on SEResNet but also on Mobile architecture EfficientNet (Tan and Le 2019).

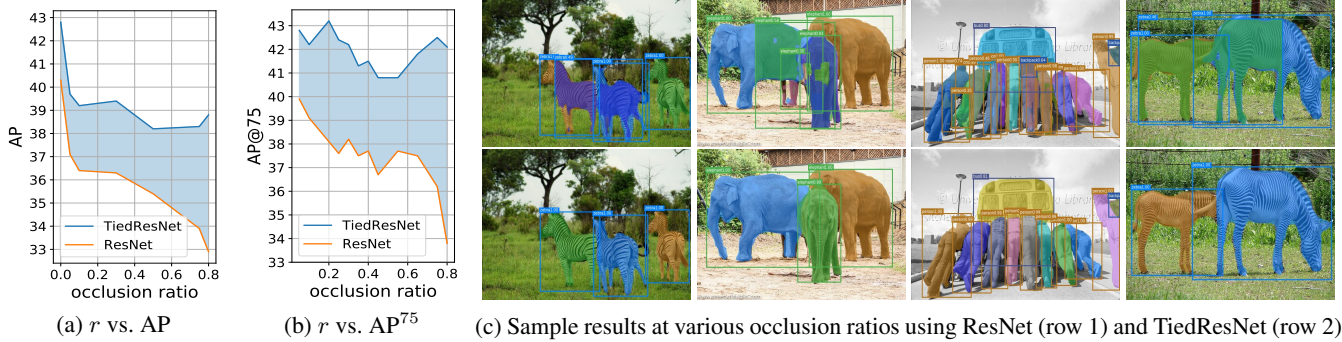


Figure 7: We evaluate TiedResNet and ResNet **performance on object detection task of MS-COCO with different occlusion ratio r** . AP (a) and AP at IoU = 0.75 (b) are reported. When $r = 0.8$, TiedResNet increases by 8.3% at AP⁷⁵ and 5.9% at AP, much more effective at handling highly overlapping instances. (c) TiedResNet has much fewer false positive proposals, and has a significantly better instance segmentation quality. We use Mask R-CNN as the detector.

model	params(M)	GFlops	top-1(%)	top-5(%)
ResNet50 (He et al. 2016)				
baseline	25.6	4.2	76.2	92.9
TiedResNet50-S	13.9 (54%)	2.5 (60%)	76.3	92.9
TiedResNet50	22.0 (86%)	4.4 (105%)	77.6	93.6
ResNet101 (He et al. 2016)				
baseline	44.6	7.9	77.4	93.6
TiedResNet101-S	24.0 (54%)	4.8 (61%)	77.7	93.8
TiedResNet101	39.4 (88%)	8.6 (109%)	78.8	94.2
ResNeXt101-32×8d (Xie et al. 2017)				
baseline	88.8	16.5	79.3	94.5
TiedResNeXt101-S	64.0 (65%)	14.6 (78%)	79.3	94.5
SENet101 (Hu, Shen, and Sun 2018)				
baseline	49.1	7.9	77.6	93.9
baseline \ddagger	49.1	7.9	78.3	94.2
TiedSENet101-S	26.4 (54%)	5.2 (66%)	79.0	94.5
TiedSENet101-S \ddagger	26.4 (54%)	5.2 (66%)	80.9	95.3
TiedSENet101	41.8 (85%)	9.1 (115%)	79.8	94.8
ResNeSt-50-fast (Zhang et al. 2020)				
baseline \ddagger	27.5	4.4	78.6	93.9
TiedResNeSt50-S	16.5 (60%)	3.6 (82%)	78.8	94.6
VS. pruning methods and Mobile nets (large model version)				
Taylor-FO-BN	14.2	2.3	74.5	-
ShuffleNet-50 \dagger	-	2.3	74.8	-
GhostNet-50 ($s=2$)	13.0	2.2	75.0	92.3
TiedResNet50-S	13.9	2.5	76.3	92.9

Table 1: **Recognition accuracy and model size comparison on ImageNet-1k**. The integration of TBC/TFC/TGC can obtain consistent performance improvements to various backbone networks. TiedResNet-S even greatly surpasses current SOTA pruning methods Taylor-FO-BN-ResNet50 (Molchanov et al. 2019) and Mobile architecture GhostNet (large model version) (Han et al. 2020). These results prove that TBC makes more efficient use of parameters. Baselines are copied from Pytorch model zoo, their TBC versions are trained for 100 epochs on 8 2080Ti GPUs to make fair comparisons, unless otherwise noticed. \dagger denotes: trained with larger epochs, label smoothing, cosine learning scheduler and heavier data augmentation. \ddagger denotes: re-implemented results with released codes, standard data augmentations and 100 training epochs.

framework	backbone	#params (M)	AP ^{mask}
Mask R-CNN	ResNet50	25.6	31.5
Mask R-CNN	TiedResNet50-S	13.9	32.5
Mask R-CNN	TiedResNet50	22.0	33.6

Table 2: Comparison on **instance segmentation task of Cityscapes val** set and number of parameters for backbone networks, with Mask R-CNN (He et al. 2017) as detector.

model	B	top-1 (%)	top-5 (%)	#params (ratio)
<i>SEResNet-50</i> , model params = 28.1M				
w/ SE	-	76.71	93.38	2.53M (100%)
w/ SE \ddagger	-	77.08	93.51	2.53M (100%)
w/ TiedSE	2	77.07	93.53	0.64M (25%)
w/ TiedSE	4	77.11	93.52	0.16M (6.4%)
w/ TiedSE	8	77.09	93.52	0.04M (1.6%)
<i>EfficientNet-B0</i> , model params = 5.3M				
w/ SE	-	77.1	93.3	0.65M (100%)
w/ TiedSE	2	77.3	93.4	0.16M (25%)
w/ TiedSE	4	77.1	93.3	0.04M (6.4%)

Table 3: Comparison on #params of **attention module SE/TiedSE** with various backbones and their recognition accuracy on ImageNet-1k. Performance with different hyper-parameters B is investigated. Using only 1.6% (6.4%) of the parameters, the performance of TiedSE is better than SE on SEResNet50 (EfficientNet-B0). \ddagger denotes our re-implementation results.

Results of TiedGCB. Global context blocks (GCB) (Cao et al. 2019) enhance segmentation and detection predictions with global context modeling and long-range dependencies. GCB integrated with TBC can significantly reduce the number of parameters without losing performance. Table 4 shows that TiedGCB achieves 1.8% and 1.4% gain in AP^{mask} and AP^{bbox} respectively, with 16 \times parameters reduction. Although group convolution can reduce parameters by 2 \times , as each GC filter only sees a subset of features, the ability to model cross-channel dependencies is also reduced, losing AP^{mask} and AP^{bbox} by 0.4%.

framework	B	AP ^{bbox}	AP ^{bbox} ₅₀	AP ^{mask}	AP ^{mask} ₅₀	#params
Mask R-CNN	-	37.3	59.0	34.2	55.9	-
+GCB	-	38.9	61.0	35.5	57.6	10M (100%)
+TiedGCB	2	39.1	61.0	35.6	57.6	2.5M (25%)
+TiedGCB	4	38.6	60.8	35.2	57.2	1.3M (13%)

Table 4: Comparison on #params of **attention module GCB/TiedGCB** (Cao et al. 2019) and their performance on object detection and instance segmentation tasks of MS-COCO *val-2017*. The effects of different B are studied here. Result of GCB with group convolution is also compared.

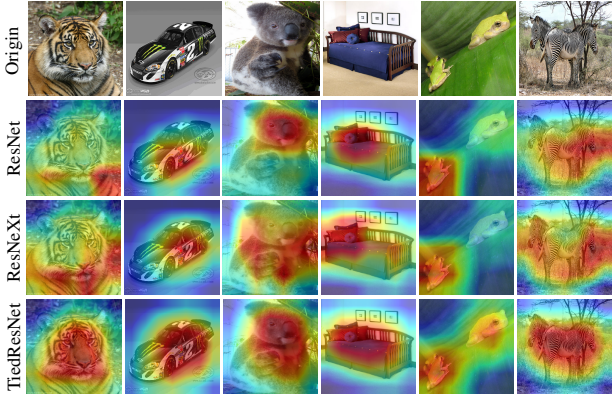


Figure 8: **Grad-CAM visualization** comparison among ResNet50, ResNeXt50 and TiedResNet50 for images in Row 1. The grad-CAM (Selvaraju et al. 2017) is calculated for the last convolutional output.

model	setting	params	GFlops	top-1	top-5
TiedResNet-50	2s×48w	23.8	4.4	77.27	93.53
TiedResNet-50	4s×32w	22.0	4.4	77.61	93.62
TiedResNet-50	6s×24w	23.0	4.6	77.37	93.66
TiedResNet-50	8s×18w	23.8	4.4	77.21	93.54

Table 5: Ablation study on **splits number** and **base width of each split**. Accuracies (%) on ImageNet-1k are listed.

mixer	top-1 acc.	top-5 acc.	#params (M)
element-sum	77.61%	93.62%	22.0
concatenate	77.65%	93.64%	26.7

Table 6: Ablation study on **fusion method** of mixer module.

Ablation Studies

Influence of split number. As investigated in (Zeiler and Fergus 2014; Bau et al. 2017; Xu et al. 2015), the proportions of units/filters that correspond to various visual concepts, such as color, texture, objects, part, scene, edge and material, are different with a variety of levels of interpretability (Agrawal, Carreira, and Malik 2015; Bau et al. 2017). It may be useful to group different functional filters together for different levels of sharing. In Table 5, we split all the channels in the 3×3 convolutional layer into s splits. Each split has base width of w , and B is 1,2,4,8 separately for the four 3×3 TBC layers in $4s \times 32w$ settings. In Table 5, the best performance and model complexity trade-off can be reached at $4s \times 32w$. Table 5 also shows the necessity of

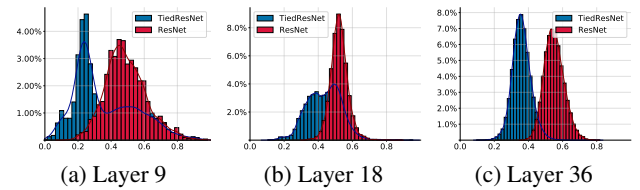


Figure 9: Histograms of pairwise filter similarity.

splitting input feature maps into several chunks, when there are only 2 splits, top-1 accuracy will drop 0.4%.

Mixer module in TiedBottleneck. Since we split the input feature map into several splits, the inter-dependency across these splits is missed. To track the inter-dependency, a mixer is used to aggregate cross-split information. Several fusion methods are investigated in Table 6. Using concatenation reaches the best accuracy, but it introduces much more parameters. We thus choose elementwise-sum as the fusion function as a trade-off between accuracy and model size.

Filter similarity. We use ImageNet pre-trained ResNet50 and TiedResNet50-S to compare the cosine filter similarity at different layers. Pairwise cosine similarity between filters’ guided back-propagation patterns (Springenberg et al. 2014) averaged in 1000 ImageNet *val* split are used to generate these histograms. As in Figure 9, axis x is the cosine similarity and axis y is the probability density. Compared with VGG(Simonyan and Zisserman 2014), ResNet(He et al. 2016) has less redundancy, and our TiedResNet has the least similarity and thus removes most redundancy throughout the depth layers, which validates our hypothesis and motivation.

Grad-CAM visualization. To provide a qualitative comparison among different backbone networks, we apply grad-CAM (Selvaraju et al. 2017) using images from ImageNet. Grad-CAM uses the gradient information flowing into the last convolutional layer of the CNN to understand each neuron. The resulting localization map highlights important regions in the image for predicting the concept and reflects the network’s ability to utilize information in the target object area. Fig.A.1 shows TiedResNet focusing on target objects more properly than ResNet and ResNetX, suggesting that the performance boost comes from accurate attention and noise reduction of irrelevant clutters.

This property is very useful for object detection and instance segmentation, as these tasks require the network to focus more accurately on the target region and aggregate features from it. Incorrect attention to the target area will also lead to a large number of false positive proposals (Fig.7c).

Summary

We propose Tied Block Convolution(TBC) that shares the same thinner filter over equal blocks of channels and produces multiple responses with a single filter. The concept of TBC can also be extended to group convolution and fully connected layers, and can be applied to various backbone networks and attention modules, with consistent performance improvements to the baseline. TBC-based TiedResNet also surpasses baselines with much higher parameter usage efficiency and better capability of detecting objects under severe occlusion.

References

- Agrawal, P.; Carreira, J.; and Malik, J. 2015. Learning to see by moving. In *Proceedings of the IEEE International Conference on Computer Vision*, 37–45.
- Bau, D.; Zhou, B.; Khosla, A.; Oliva, A.; and Torralba, A. 2017. Network dissection: Quantifying interpretability of deep visual representations. In *Proceedings of the IEEE Conference on Computer Vision and Pattern Recognition*, 6541–6549.
- Cai, Z.; and Vasconcelos, N. 2018. Cascade r-cnn: Delving into high quality object detection. In *Proceedings of the IEEE conference on computer vision and pattern recognition*, 6154–6162.
- Cao, Y.; Xu, J.; Lin, S.; Wei, F.; and Hu, H. 2019. GC-Net: Non-local Networks Meet Squeeze-Excitation Networks and Beyond. *arXiv preprint arXiv:1904.11492*.
- Carreira, J.; and Zisserman, A. 2017. Quo vadis, action recognition? a new model and the kinetics dataset. In *proceedings of the IEEE Conference on Computer Vision and Pattern Recognition*, 6299–6308.
- Chen, K.; Wang, J.; Pang, J.; Cao, Y.; Xiong, Y.; Li, X.; Sun, S.; Feng, W.; Liu, Z.; Xu, J.; Zhang, Z.; Cheng, D.; Zhu, C.; Cheng, T.; Zhao, Q.; Li, B.; Lu, X.; Zhu, R.; Wu, Y.; Dai, J.; Wang, J.; Shi, J.; Ouyang, W.; Loy, C. C.; and Lin, D. 2019. MMDetection: Open MMLab Detection Toolbox and Benchmark. *arXiv preprint arXiv:1906.07155*.
- Chen, L.-C.; Papandreou, G.; Kokkinos, I.; Murphy, K.; and Yuille, A. L. 2017. DeepLab: Semantic image segmentation with deep convolutional nets, atrous convolution, and fully connected crfs. *IEEE transactions on pattern analysis and machine intelligence* 40(4): 834–848.
- Chen, L.-C.; Zhu, Y.; Papandreou, G.; Schroff, F.; and Adam, H. 2018. Encoder-decoder with atrous separable convolution for semantic image segmentation. In *Proceedings of the European conference on computer vision (ECCV)*, 801–818.
- Cordts, M.; Omran, M.; Ramos, S.; Rehfeld, T.; Enzweiler, M.; Benenson, R.; Franke, U.; Roth, S.; and Schiele, B. 2016. The cityscapes dataset for semantic urban scene understanding. In *Proceedings of the IEEE conference on computer vision and pattern recognition*, 3213–3223.
- Deng, J.; Dong, W.; Socher, R.; Li, L.-J.; Li, K.; and Fei-Fei, L. 2009. Imagenet: A large-scale hierarchical image database. In *2009 IEEE conference on computer vision and pattern recognition*, 248–255. Ieee.
- Everingham, M.; Eslami, S. M. A.; Van Gool, L.; Williams, C. K. I.; Winn, J.; and Zisserman, A. 2015. The Pascal Visual Object Classes Challenge: A Retrospective. *International Journal of Computer Vision* 111(1): 98–136.
- Girshick, R. 2015. Fast r-cnn. In *Proceedings of the IEEE international conference on computer vision*, 1440–1448.
- Han, K.; Wang, Y.; Tian, Q.; Guo, J.; Xu, C.; and Xu, C. 2020. GhostNet: More features from cheap operations. In *Proceedings of the IEEE/CVF Conference on Computer Vision and Pattern Recognition*, 1580–1589.
- He, K.; Gkioxari, G.; Dollár, P.; and Girshick, R. 2017. Mask r-cnn. In *Proceedings of the IEEE international conference on computer vision*, 2961–2969.
- He, K.; Zhang, X.; Ren, S.; and Sun, J. 2016. Deep residual learning for image recognition. In *Proceedings of the IEEE conference on computer vision and pattern recognition*, 770–778.
- Howard, A. G.; Zhu, M.; Chen, B.; Kalenichenko, D.; Wang, W.; Weyand, T.; Andreetto, M.; and Adam, H. 2017. Mobilenets: Efficient convolutional neural networks for mobile vision applications. *arXiv preprint arXiv:1704.04861*.
- Hu, J.; Shen, L.; and Sun, G. 2018. Squeeze-and-excitation networks. In *Proceedings of the IEEE conference on computer vision and pattern recognition*, 7132–7141.
- Ji, S.; Xu, W.; Yang, M.; and Yu, K. 2012. 3D convolutional neural networks for human action recognition. *IEEE transactions on pattern analysis and machine intelligence* 35(1): 221–231.
- Kirillov, A.; Girshick, R.; He, K.; and Dollár, P. 2019. Panoptic feature pyramid networks. In *Proceedings of the IEEE Conference on Computer Vision and Pattern Recognition*, 6399–6408.
- Krizhevsky, A.; Sutskever, I.; and Hinton, G. E. 2012. Imagenet classification with deep convolutional neural networks. In *Advances in neural information processing systems*, 1097–1105.
- Lin, T.-Y.; Goyal, P.; Girshick, R.; He, K.; and Dollár, P. 2017. Focal loss for dense object detection. In *Proceedings of the IEEE international conference on computer vision*, 2980–2988.
- Lin, T.-Y.; Maire, M.; Belongie, S.; Hays, J.; Perona, P.; Ramanan, D.; Dollár, P.; and Zitnick, C. L. 2014. Microsoft coco: Common objects in context. In *European conference on computer vision*, 740–755. Springer.
- Long, J.; Shelhamer, E.; and Darrell, T. 2015. Fully convolutional networks for semantic segmentation. In *Proceedings of the IEEE conference on computer vision and pattern recognition*, 3431–3440.
- Ma, N.; Zhang, X.; Zheng, H.-T.; and Sun, J. 2018. Shufflenet v2: Practical guidelines for efficient cnn architecture design. In *Proceedings of the European Conference on Computer Vision (ECCV)*, 116–131.
- Molchanov, P.; Mallya, A.; Tyree, S.; Frosio, I.; and Kautz, J. 2019. Importance estimation for neural network pruning. In *Proceedings of the IEEE Conference on Computer Vision and Pattern Recognition*, 11264–11272.
- Ren, S.; He, K.; Girshick, R.; and Sun, J. 2015. Faster r-cnn: Towards real-time object detection with region proposal networks. In *Advances in neural information processing systems*, 91–99.
- Selvaraju, R. R.; Cogswell, M.; Das, A.; Vedantam, R.; Parikh, D.; and Batra, D. 2017. Grad-cam: Visual explanations from deep networks via gradient-based localization. In *Proceedings of the IEEE international conference on computer vision*, 618–626.

- Simonyan, K.; and Zisserman, A. 2014. Very deep convolutional networks for large-scale image recognition. *arXiv preprint arXiv:1409.1556*.
- Springenberg, J. T.; Dosovitskiy, A.; Brox, T.; and Riedmiller, M. 2014. Striving for simplicity: The all convolutional net. *arXiv preprint arXiv:1412.6806*.
- Szegedy, C.; Liu, W.; Jia, Y.; Sermanet, P.; Reed, S.; Anguelov, D.; Erhan, D.; Vanhoucke, V.; and Rabinovich, A. 2015. Going deeper with convolutions. In *Proceedings of the IEEE conference on computer vision and pattern recognition*, 1–9.
- Tan, M.; and Le, Q. V. 2019. Efficientnet: Rethinking model scaling for convolutional neural networks. *arXiv preprint arXiv:1905.11946*.
- Wang, J.; Sun, K.; Cheng, T.; Jiang, B.; Deng, C.; Zhao, Y.; Liu, D.; Mu, Y.; Tan, M.; Wang, X.; et al. 2019. Deep high-resolution representation learning for visual recognition. *arXiv preprint arXiv:1908.07919*.
- Wang, L.; Xiong, Y.; Wang, Z.; Qiao, Y.; Lin, D.; Tang, X.; and Van Gool, L. 2016. Temporal segment networks: Towards good practices for deep action recognition. In *European conference on computer vision*, 20–36. Springer.
- Wang, X.; Girshick, R.; Gupta, A.; and He, K. 2018. Non-local neural networks. In *Proceedings of the IEEE Conference on Computer Vision and Pattern Recognition*, 7794–7803.
- Xie, S.; Girshick, R.; Dollár, P.; Tu, Z.; and He, K. 2017. Aggregated residual transformations for deep neural networks. In *Proceedings of the IEEE conference on computer vision and pattern recognition*, 1492–1500.
- Xu, K.; Ba, J.; Kiros, R.; Cho, K.; Courville, A.; Salakhudinov, R.; Zemel, R.; and Bengio, Y. 2015. Show, attend and tell: Neural image caption generation with visual attention. In *International conference on machine learning*, 2048–2057.
- Zeiler, M. D.; and Fergus, R. 2014. Visualizing and understanding convolutional networks. In *European conference on computer vision*, 818–833. Springer.
- Zhang, H.; Wu, C.; Zhang, Z.; Zhu, Y.; Zhang, Z.; Lin, H.; Sun, Y.; He, T.; Mueller, J.; Manmatha, R.; et al. 2020. Resnest: Split-attention networks. *arXiv preprint arXiv:2004.08955*.
- Zhang, X.; Zhou, X.; Lin, M.; and Sun, J. 2018. Shufflenet: An extremely efficient convolutional neural network for mobile devices. In *Proceedings of the IEEE Conference on Computer Vision and Pattern Recognition*, 6848–6856.

Tied Block Convolution: Leaner and Better CNNs with Shared Thinner Filters

Supplementary Materials

Detailed Results on Object Detection and Instance Segmentation

Here we provide **detailed results of experimented backbones and frameworks on object detection and instance segmentation tasks** of MS-COCO (Lin et al. 2014) in Table A.1 and Table A.2. Average Precision (AP) across IoU thresholds from 0.5 to 0.95 with an interval of 0.05 and AP under various qualities and scales are reported. All experiments are conducted on mmdetection v1.0 codebase (Chen et al. 2019).

Regardless of the type and the performance of the experimented detector, TiedResNet consistently outperforms ResNet by more than 2%, and has a higher efficiency of parameter usage. The light version of TiedResNet even increase the performance by 1.2% with about 2 times parameter reduction. In addition, the improvements in detection and instance segmentation tasks (about 2.5%) are usually higher than the improvements in recognition task (about 1.5%). In comparison, ResNeXt’s improvements in recognition and detection tasks are similar, that is, about 1.4%. This indicates that TiedResNet is a more suitable backbone for detection and has a stronger localization capability.

We also experiment our **TBC/TGC/TFC on multiple backbones**, with Mask R-CNN as a detector, to prove the effectiveness and universality of proposed operators on de-

tction and instance segmentation tasks. All these backbones and their counterparts are pretrained on ImageNet for 100 epochs to make fair comparisons. Similar to the observation in the ImageNet recognition task, by integrating TBC/TGC/TFC into multiple backbones, consistent improvements are obtained.

Additional Grad-CAM visualization Results

Additional visualization results with Grad-CAM (Selvaraju et al. 2017) is shown in Figure A.1. As an algorithm to create a high-resolution class-discriminative visualization, Grad-CAM could illustrate the network’s ability to utilize information in the target object area. Figure A.1 shows TiedResNet localizing target instances more accurately than baselines, suggesting that the performance boost in object detection and instance segmentation tasks comes from precise attention and noise reduction of irrelevant clutters.

Sample Results

The sample results of object detection and instance segmentation tasks on multiple datasets, including Cityscapes (Cordts et al. 2016), Pascal VOC (Everingham et al. 2015) and MS-COCO (Lin et al. 2014), are visualized in Figure A.2. Our TiedResNet shows strong capability of handling highly overlapping instances.

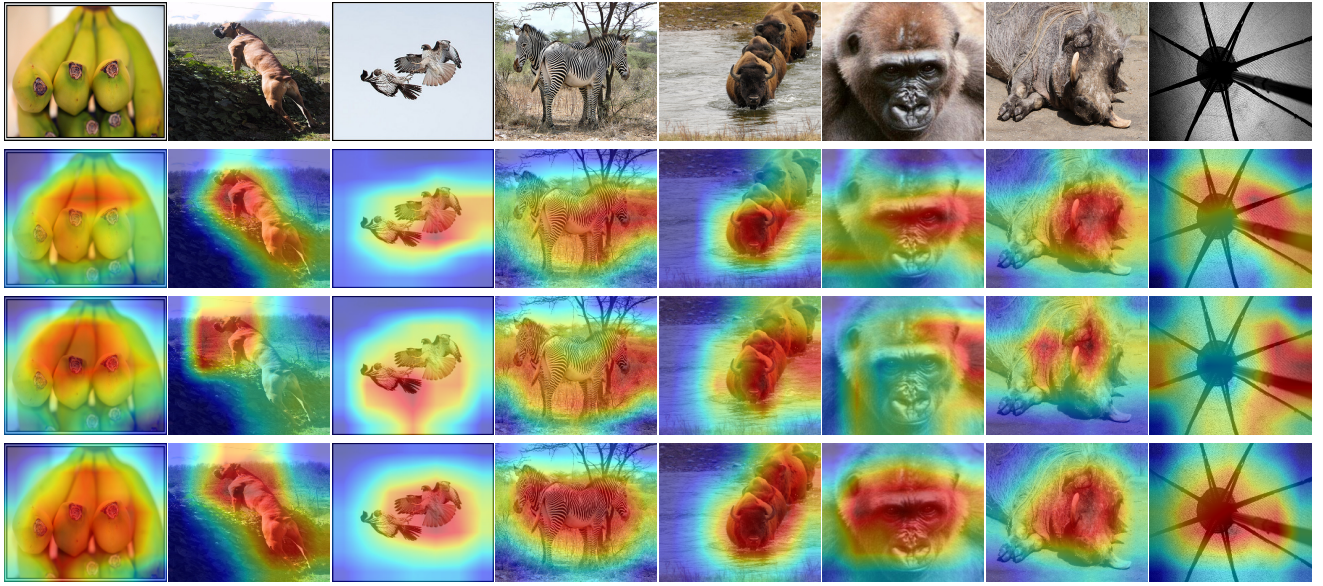


Figure A.1: Additional Grad-CAM (Selvaraju et al. 2017) visualization comparison among ResNet50, ResNeXt50 and TiedResNet50 in Rows 2-4 respectively for images in Row 1. The grad-CAM is calculated for the last convolutional output.

Backbone	#param	LS=1×				LS=2×/20e			
		AP	AP _S	AP _M	AP _L	AP	AP _S	AP _M	AP _L
RetinaNet (Lin et al. 2017)									
ResNet-50	25.6M	35.6	20.0	39.6	46.8	36.4	19.3	39.9	48.9
TiedResNet-50-S	13.9M	36.8	21.0	40.8	48.1	37.5	20.3	41.2	50.1
<i>vs. baseline</i>	↓11.7M	+1.2	+1.0	+1.2	+1.3	+1.1	+1.0	+1.3	+1.2
TiedResNet-50	22.0M	37.7	21.3	41.8	49.5	38.6	21.3	42.3	51.5
<i>vs. baseline</i>	↓3.6M	+2.1	+1.3	+2.2	+2.7	+2.2	+2.0	+2.4	+2.6
ResNet-101	44.6M	37.7	21.1	42.2	49.5	38.1	20.2	41.8	50.8
TiedResNet-101-S	24.0M	39.8	22.4	44.4	52.2	39.1	20.9	42.6	52.1
<i>vs. baseline</i>	↓20.6M	+1.2	+0.6	+1.0	+1.8	+1.0	+0.7	+0.8	+1.3
TiedResNet-101	39.4M	39.8	22.4	44.4	52.2	40.5	22.9	44.8	52.7
<i>vs. baseline</i>	↓5.2M	+2.2	+1.4	+2.0	+2.8	+2.4	+2.7	+3.0	+1.9
Cascade R-CNN (Cai and Vasconcelos 2018)									
ResNet-101	44.6M	40.4	21.5	43.7	53.8	42.5	23.7	46.1	56.9
TiedResNet-101-S	24.0M	41.5	22.5	44.9	54.7	43.8	24.8	47.4	58.4
<i>vs. baseline</i>	↓22.6M	+1.1	+1.0	+1.2	+0.9	+1.3	+1.1	+1.3	+1.5
TiedResNet-101	39.4M	42.7	22.8	46.6	57.0	44.8	25.3	49.0	59.2
<i>vs. baseline</i>	↓5.2M	+2.3	+1.3	+2.9	+3.2	+2.3	+1.6	+2.9	+2.3

Table A.1: #params of backbones vs. their Average Precision on object detection task of MS-COCO *val-2017*. LS denotes learning schedule. Baseline are obtained from (Chen et al. 2019). We experiment TBC on various detectors, including single stage detector RetinaNet (Lin et al. 2017) and SOTA two-stage detector Cascade R-CNN (Cai and Vasconcelos 2018). Consistent performance improvements can be observed. Reported results are used to plot Figure 6(a) and Figure 6(b) of our submission.

Backbone	LS	#param	Object Detection				Instance Segmentation			
			AP	AP _S	AP _M	AP _L	AP	AP _S	AP _M	AP _L
Mask R-CNN (He et al. 2017)										
ResNet-50	2×	25.6M	38.5	22.6	42.0	50.5	35.1	16.7	37.7	52.0
TiedResNet-50-S	2×	13.9M	39.6	23.0	43.3	51.3	36.2	17.0	38.8	52.8
<i>vs. baseline</i>	-	↓11.7M	+1.1	+0.4	+1.3	+0.8	+1.1	+0.3	+1.1	+0.8
TiedResNet-50	2×	22.0M	40.9	24.0	44.7	53.6	37.0	17.4	39.9	54.6
<i>vs. baseline</i>	-	↓3.6M	+2.4	+1.4	+2.7	+3.1	+1.9	+0.7	+2.2	+2.6
ResNet-101	2×	44.6M	40.3	22.2	44.8	52.9	36.5	16.3	39.7	54.6
TiedResNet-101-S	2×	24.0M	41.7	24.1	45.8	54.3	37.5	17.9	40.5	55.0
<i>vs. baseline</i>	-	↓20.6M	+1.4	+1.9	+1.0	+1.4	+1.0	+1.6	+0.8	+0.4
TiedResNet-101	2×	39.4M	42.8	24.2	46.8	57.2	38.4	18.2	41.5	57.0
<i>vs. baseline</i>	-	↓5.2M	+2.5	+2.0	+2.0	+4.3	+1.9	+1.9	+0.8	+3.4
SENet-101	2×	49.1M	41.1	23.3	45.6	54.5	37.2	17.3	40.2	55.1
TiedSENet-101-S	2×	22.8M	42.4	24.9	46.6	55.7	38.2	18.6	41.1	56.1
<i>vs. baseline</i>	-	↓5.2M	+1.3	+1.6	+1.0	+1.2	+1.0	+1.3	+0.9	+1.0
TiedSENet-101	2×	41.8M	43.4	25.3	48.2	58.4	38.9	19.1	42.2	58.3
<i>vs. baseline</i>	-	↓7.3M	+2.3	+2.0	+2.6	+3.9	+1.7	+1.8	+2.0	+3.2
ResNeXt-101-32×8d	2×	88.8M	42.8	24.5	46.9	55.7	38.3	16.7	37.7	52.0
TiedResNeXt-101-32×8d	2×	64.0M	44.0	26.0	47.6	56.5	39.2	17.9	38.7	52.7
<i>vs. baseline</i>	-	↓24.8M	+1.2	+1.5	+0.7	+0.8	+0.9	+1.2	+1.0	+0.7
Cascade Mask R-CNN (Cai and Vasconcelos 2018)										
ResNet-50	20e	25.6M	42.3	23.7	45.7	56.4	36.6	17.3	39.0	53.9
TiedResNet-50	20e	22.0M	44.7	25.8	47.9	59.3	38.4	18.7	40.9	56.5
<i>vs. baseline</i>	-	↓3.6M	+2.4	+2.1	+2.2	+2.9	+1.8	+1.6	+1.9	+2.6
ResNet-101	20e	44.6M	43.3	24.4	46.9	58.0	37.6	17.3	40.4	56.2
TiedResNet-101-S	20e	24.0M	44.5	25.2	48.4	59.0	38.6	18.4	41.6	56.8
<i>vs. baseline</i>	-	↓22.6M	+1.2	+0.8	+1.6	+1.0	+1.0	+1.1	+1.2	+0.6
TiedResNet-101	20e	39.4M	45.6	26.4	49.5	60.7	39.3	19.1	42.4	58.0
<i>vs. baseline</i>	-	↓5.2M	+2.3	+2.0	+2.6	+2.7	+1.7	+1.8	+2.0	+2.2

Table A.2: #params of backbones vs. their Average Precision on object detection and instance segmentation tasks of MS-COCO *val-2017*. LS denotes learning rate schedule. We experiment TBC on different kinds of backbone networks, including ResNet, ResNeXt and SENet. Consistent performance improvements can be obtained. *Our TiedResNet-101 (with TBC) not only outperforms ResNet-101 counterpart but also achieves comparable performance with ResNeXt-101-32-×8d (with Group Convolution) with only 44% parameters..* Results in this table was used to plot Figure 6(c) and Figure 6(d) of our submission



Figure A.2: Sample results of object detection and instance segmentation on Cityscapes *val* (Cordts et al. 2016) (ROW 1, 2), Pascal VOC *test-2007* (Everingham et al. 2015) (ROW 3, 4, 5) and MS-COCO *val-2017* (Lin et al. 2014) (ROW 5, 6, 7) splits. We choose Mask R-CNN with TiedResNet-50 as a detection framework for Cityscapes and MS-COCO datasets and use Faster R-CNN with TiedResNet-50 as a detector for Pascal VOC dataset. All positive proposals with confidence scores greater than 0.05 are visualized here. Although many instances are highly overlapping with each other, our network can still distinguish them clearly and make high-quality bounding box proposals and segmentation masks.